Neural Computing and Applications (2021) 33:3417–3436
https://doi.org/10.1007/s00521-020-05187-w

ORIGINAL ARTICLE

Integrated intelligent computing paradigm for nonlinear multi-singular third-order Emden–Fowler equation

Zulqurnain Sabir[1] · Muhammad Umar[1] · Juan L. G. Guirao[2] · Muhammad Shoaib[3] · Muhammad Asif Zahoor Raja[4]

Received: 22 August 2019 / Accepted: 11 July 2020 / Published online: 25 July 2020

Abstract
In this study, an advance computational intelligence scheme is designed and implemented to solve third-order nonlinear multiple singular systems represented with Emden–Fowler differential equation (EFDE) by exploiting the efficacy of artificial neural networks (ANNs), genetic algorithms (GAs) and active-set algorithm (ASA), i.e., ANN–GA–ASA. In the scheme, ANNs are used to discretize the EFDE for formulation of mean squared error-based fitness function. The optimization task for ANN models of nonlinear multi-singular system is performed by integrated competency GA and ASA. The efficiency of the designed ANN–GA–ASA is examined by solving five different variants of the singular model to check the effectiveness, reliability and significance. The statistical investigations are also performed to authenticate the precision, accuracy and convergence.

Keywords Nonlinear Emden–Fowler equation · Artificial neural networks · Statistical analysis · Genetic algorithms · Singular systems · Active-set algorithm · Hybrid computing

1 Introduction

Astrophysicist Lane [1] and Emden [2] first time introduced nonlinear singular Lane–Emden model working on thermal performance of a spherical cloud of gas and classical law of thermodynamics [3]. The singular models designate a variety of phenomena in physical science [4], density profile of gaseous star [5], catalytic diffusion reactions [6], isothermal gas spheres [7], catalytic diffusion reactions [6], stellar structure [8], electromagnetic theory [9], mathematical physics [10], classical and quantum mechanics [11], oscillating magnetic fields [12], isotropic continuous media [13], dusty fluid models [14] and morphogenesis [15]. To find the solution, these singular models are always very challengeable and hard to handle due to the singularity at the origin. The generic form on of such model represented with third-order nonlinear Emden–Fowler equation is written as [16]:

$$y'''(t) + \left(\frac{2p}{t}\right)y''(t) + \frac{p(p-1)}{t^2}y'(t) + f(t)g(y) = 0, \qquad (1)$$
$$y(0) = y_0,\ y'(0) = 0,\ y''(0) = 0.$$

There are only few numerical and analytic existing techniques to tackle such nonlinear singular models (1). To

✉ Juan L. G. Guirao
juan.garcia@upct.es

Zulqurnain Sabir
zulqurnain_maths@hu.edu.pk

Muhammad Umar
umar_maths@hu.edu.pk; humar922015@gmail.com

Muhammad Shoaib
dr.shoaib@cuiatk.edu.pk

Muhammad Asif Zahoor Raja
Muhammad.asif@ciit-attock.edu.pk

1 Department of Mathematics and Statistics, Hazara University, Mansehra, Pakistan

2 Department of Applied Mathematics and Statistics, Technical University of Cartagena, Hospital de Marina, 30203 Cartagena, Spain

3 Department of Mathematics, COMSATS University Islamabad, Attock Campus, Attock 43600, Pakistan

4 Department of Electrical and Computer Engineering, COMSATS University Islamabad, Attock Campus, Attock 43600, Pakistan

mention few reported techniques to solve the singular models represented with differential equations include Shawagfeh [17] used the Adomian decomposition method (ADM), Wazwaz [18] also applied ADM to avoid the difficulty of singularity, Liao [19] applied an analytic algorithm to avoid the singularity, He and Ji [20] developed a numerical scheme based on Taylor series, Nouh [21] applied power series solution by using Pade approximation technique as well as Euler-Abel transformation and Mandelzweig and along with Tabakin [22] developed Bellman and Kalabas quasi-linearization method. All these techniques have their own performance, accuracy and efficiency, as well as inadequacies over one another. Beside these deterministic procedures, numerical solvers based on heuristic computing paradigm look promising to be incorporated in the domain of nonlinear singular systems.

The considerable potential of heuristic computing paradigm based on stochastic numerical solvers is exploited for solving linear/nonlinear systems by manipulating the universal approximation competency of artificial neural networks (ANNs) optimized with local/global search methodologies [23–25]. Few recent applications of paramount significance include Thomas–Fermi atom's model [26], prey-predator models [27], plasma physics problems [28], models of fractional ordinary differential equations [29], model of heartbeat dynamics [30], linear fractional cable equation [31], machines [32], control systems [33], cell biology [34], power [35] and energy [36]. The intention of the present study is to present the detail study of the singular Emden–Fowler model along with numerical results for better system understanding using the stochastic technique.

The aim of the present study is to find the solution of Eq. (1) by integrated intelligent computing paradigm based on the artificial neural networks (ANNs) optimized with genetic algorithms (GAs) refined by the active-set algorithm (ASA), i.e., ANN–GA–ASA. The major features of the proposed solver ANN–GA–ASA are briefly given below:

- A novel application of integrated intelligent computing paradigm ANN–GA–ASA is presented for finding the solution of nonlinear multi-singular models governed with third-order nonlinear Emden–Fowler equation.
- Consistently matching outcomes of the proposed ANN–GA–ASA with reference solutions for different variant of nonlinear Emden–Fowler system established the worth of the solver in terms of accuracy and convergence.
- Validation of the performance is ascertained through statistical observations on multiple execution of ANN–GA–ASA in terms of mean absolute deviation (MAD), Theil's inequality coefficient (TIC) and Nash–Sutcliffe efficiency (NSE) performance indices.
- Beside provision of accurate solution of nonlinear Emden–Flower differential system, smooth implementation, ease in understanding, stability, applicability and robustness are other valuable promises.

Rest of the paper is organized as follows: proposed framework of stochastic solver ANN–GA–ASA is presented in Sect. 2, performance measures are listed at Sect. 3, result with discussions is presented in Sect. 4, while conclusions with future related works are listed Sect. 5.

2 Proposed methodology

The proposed framework as shown in Fig. 1 for presenting the solution of model (1) is divided in two portions. Firstly, by introducing the procedure for formulation of an error-based fitness function and secondly, the combination of GA-ASA is presented to optimize the fitness function for system (1).

2.1 ANN modeling

The variety of ANN models are introduced by research community for the solutions of nonlinear systems arising in application of broad fields [37–39]. The feed-forward ANN models-based procedure for approximating solutions and their respective mth order derivatives are mathematically presented as:

$$\hat{y}(t) = \sum_{j=1}^{n} \alpha_j h(\delta_j t + \beta_j), \tag{2}$$

$$\hat{y}^{(m)}(t) = \sum_{j=1}^{n} \alpha_j h^{(m)}(\delta_j t + \beta_j), \tag{3}$$

where α_j, δ_j and β_j are the respective jth components of $\boldsymbol{\alpha}$, $\boldsymbol{\delta}$ and $\boldsymbol{\beta}$ vectors, while m shows the derivative order. The log-sigmoid expression $h(t) = (1+\exp(-t))^{-1}$ and its derivative are used as an activation/transfer functions in the networks. The updated form of the above network is written as follows:

$$\hat{y}(t) = \sum_{j=1}^{n} \alpha_j \left(1 + e^{-(\delta_j t + \beta_j)}\right)^{-1}, \tag{4}$$

$$\hat{y}^{(m)}(t) = \sum_{j=1}^{n} \alpha_j \frac{d^m}{dt^m}\left(\left(1 + e^{-(\delta_j t + \beta_j)}\right)^{-1}\right). \tag{5}$$

In case of Emden–Fowler Eq. (1), the expression for high order derivative in ANN formulations is given as:

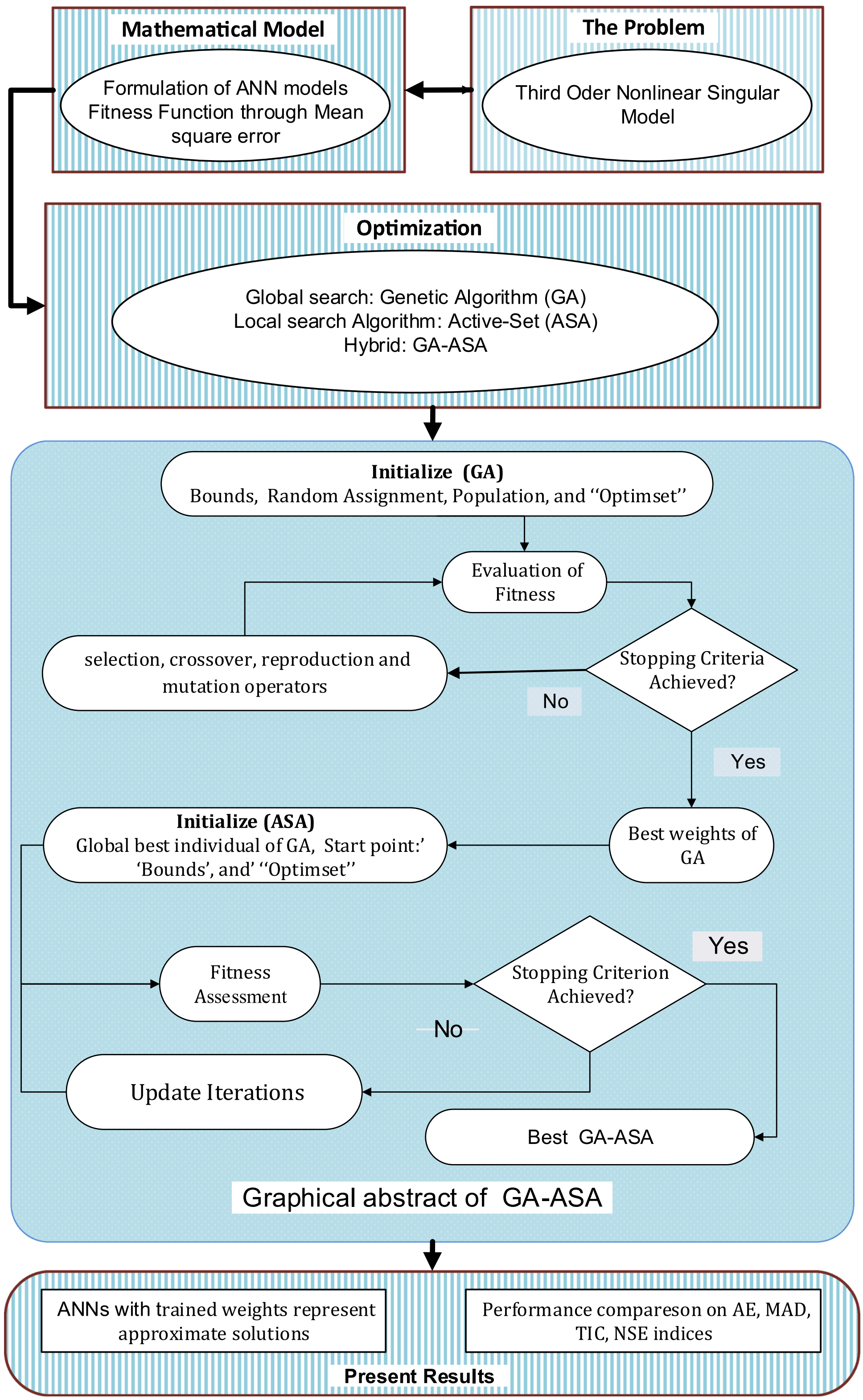

Fig. 1 Framework of proposed methodology to solve nonlinear Emden–Fowler model

$$\hat{y}'''(t) = \sum_{j=1}^{n} \alpha_j \delta_j^3 \left(\frac{6e^{-3(\delta_j t+\beta_j)}}{\left(1+e^{-(\delta_j t+\beta_j)}\right)^4} - \frac{6e^{-2(\delta_i t+\beta_i)}}{\left(1+e^{-(\delta_j t+\beta_j)}\right)^3} + \frac{e^{-(\delta_i t+\beta_i)}}{\left(1+e^{-(\delta_j t+\beta_j)}\right)^2} \right) \tag{6}$$

The networks (4) to (6) are arbitrarily combined to form the ANN architecture for nonlinear Emden–Fowler equation as shown in Fig. 2. The combination of Eqs. (4) to (6) is exploited for the fitness function formulation of Eq. (1) in mean squared error sense as:

$$\varepsilon = \varepsilon_1 + \varepsilon_2, \tag{7}$$

$$\varepsilon_1 = \frac{1}{N} \sum_{k=1}^{N} \left(\hat{y}_k''' + 2pt_k^{-1}\hat{y}_k'' + p(p-1)t_k^{-2}\hat{y}_k' + f_k g(\hat{y}_k) \right)^2, \tag{8}$$

$$\varepsilon_2 = \frac{1}{2}\left((\hat{y}_0 - A)^2 + (\hat{y}_0')^2 + (\hat{y}_0'')^2 \right), \tag{9}$$

where ε_1 and ε_2 are the fitness/error functions associated with main body of Eq. (1) and its initial conditions, respectively, while $N = 1/h,\ \hat{y}_k = \hat{y}(t_k), t_k = kh,\ f_k = f(t_k)$. An appropriate optimization procedure is adopted for learning of weight vector $W = [\boldsymbol{\alpha},\ \boldsymbol{\delta},\ \boldsymbol{\beta}]$, such that error-based fitness function (7) approaches to optimal zero value.

2.2 Optimization procedure

The weights of ANNs are trained by manipulating the strength of integrated meta-heuristic computing procedure based on GAs supported with ASA, i.e., GA-ASA. The graphical abstract of present designed methodology for solving Eq. (1) is presented in Fig. 1.

Global search efficacy of GAs, introduced by Holland in early 1970's [40, 41], is exploited for finding the weight vector W of ANN. Population formulation with candidate solution or individual in GAs is performed using the bounded real numbers. While, each candidate solution or individual has elements equal to unknown weights in ANN models. GAs operate with its fundamental operators based on selection, crossover, mutation and elitism procedures and has been used in many applications recently, for instance, solving nonlinear electric circuit models [42], emergency humanitarian logistics scheduling [43], dynamics of nonlinear Troesch's problem [44], traveling salesman problem [45], parameter estimation [46], fecal coliform predictive model [47], nonlinear nanofluidic model [48], optimization of wireless sensor network in smart grids [49], nonlinear micropolar fluid flow systems [50], recommendation systems [51] and prediction of thermal conductivity [52].

The optimized parameters of GA converge faster by the hybridization procedure with the appropriate local search method by taking global best of GAs as initial weights.

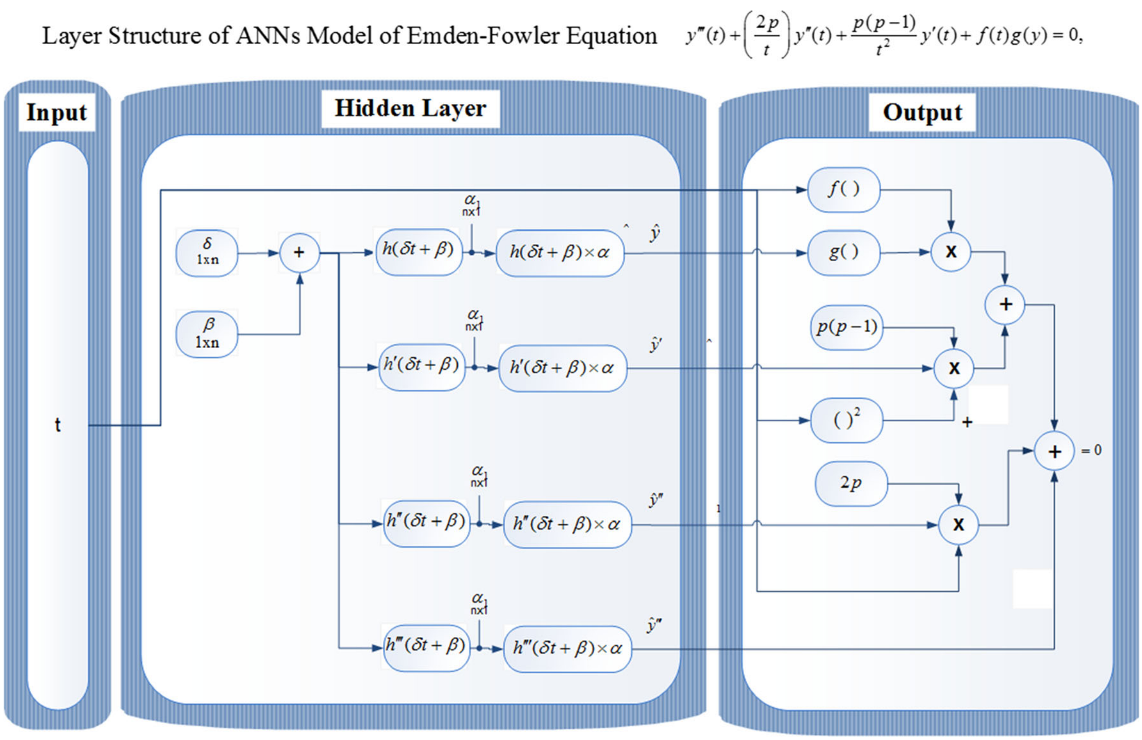

Fig. 2 ANN architecture for nonlinear third-order singular Emden–Fowler model

Therefore, efficient local search method based on active-set algorithm (ASA) is used of rapid fine tuning of parameters. Recently, ASA-based optimization is used in many applications, e.g., water distribution systems [53], solution of optimal control problems [54], distributed model predictive control [55], transportation of discrete network design bi-level problem [56] and solution of ball/sphere constrained optimization problems [57]. In the present study, the hybrid scheme based on GA-ASA is used in order to tune the decision variables for solving the third-order singular model (1). The detailed pseudocode of GA-ASA is tabulated in Table 1

Stability of proposed stochastic solver ANN–GA–ASA based on neural networks with arbitrary weights, that dependent on number of neurons in the hidden layers, is mainly carried out with the help of two procedures, i.e., theoretical analysis and stochastic analysis. In theoretical analysis, appropriate global and local conditions are derived generally with the help of problem specific Lyapunov functions [58–60], while in stochastic analysis, Monte Carlo simulation is conducted with different set of the parameters of the neural networks and results of statistical observations are used to evaluate the stability [61–63].

3 Performance measures

The performance measures of MAD, NSE and TIC are incorporated for the analysis in this study.

The mathematical expression of MAD, TIC and NSE by means of the exact/true solution y and approximate/calculated solution $\hat{y}$ are provided below:

$$\text{MAD} = \frac{1}{n}\sum_{m=1}^{n}|y_m - \hat{y}_m|, \tag{10}$$

$$\text{TIC} = \frac{\sqrt{\frac{1}{n}\sum_{m=1}^{n}(y_m - \hat{y}_m)^2}}{\left(\sqrt{\frac{1}{n}\sum_{m=1}^{n}y_m^2} + \sqrt{\frac{1}{n}\sum_{m=1}^{n}\hat{y}_m^2}\right)} \tag{11}$$

$$\text{NSE} = \left\{1 - \frac{\sum_{m=1}^{n}(y_m - \hat{y}_m)^2}{\sum_{m=1}^{n}(y_m - \bar{y}_m)^2}, \quad \bar{y}_m = \frac{1}{n}\sum_{m=1}^{n} y_m \right. \tag{12}$$

$$\text{E}_{NSE} = 1 - \text{NSE} \tag{13}$$

4 Results and discussion

The detailed results of proposed ANN–GA–ASA along with necessary interpretation are presented for five cases of nonlinear singular Emden–Fowler system (1) in this section. The stability of the proposed stochastic solver ANN–GA–ASA based on neural networks is evaluated on stochastic analysis which is performed on 100 independent runs of ANN–GA–ASA to solve nonlinear multi-singular third-order Emden–Fowler equations. Additionally, the accuracy, convergence, stability and robustness of the proposed stochastic solver ANN–GA–ASA are examined with the help of statistical observations on different performance metrics, MAD, TIC, ENSE and their global variants GMAD, GTIC and GENSE based on 100 number of independent runs of the solver. The five cases of the nonlinear singular Emden–Fowler system (1) are narrated as follows.

Case I Consider the nonlinear Emden–Fowler equation by putting $p = 1$ and $f(t)g(y) = -\frac{9}{8}(t^6 + 8)y^{-5}$ in Eq. (1), then we have:

$$\begin{aligned} & y'''(t) + \left(\frac{2}{t}\right)y''(t) - \frac{9}{8}(8 + t^6)y^{-5} = 0 \\ & y(0) = 1, \;\; y'(0) = 0, \;\; y''(0) = 0. \end{aligned} \tag{14}$$

The exact/true form of the solution of (14) is $\sqrt{1 + t^3}$, and the fitness/error function for (14) is given below:

$$\begin{aligned} \varepsilon = & \frac{1}{N}\sum_{m=1}^{N}\left(8t_m\hat{y}'''(t_m) + 16\hat{y}''(t_m) - 9t_m(t_m^6 + 8)\hat{y}^{-5}\right)^2 \\ & + \frac{1}{3}\left((\hat{y}_0 - 1)^2 + (\hat{y}'_0)^2 + (\hat{y}''_0)\right) \end{aligned} \tag{15}$$

Case II Consider the third-order Emden–Fowler model by using $p = 2$ and $f(t)g(y) = -9(3t^6 + 10t^3 + 4)y$ in Eq. (1), then we have

$$\begin{aligned} & y'''(t) + \left(\frac{4}{t}\right)y''(t) + \left(\frac{2}{t^2}\right)y'(t) - 9(4 + 10t^3 + 3t^6)y = 0 \\ & y(0) = 1, \;\; y'(0) = 0, \;\; ''(0) = 0. \end{aligned} \tag{16}$$

The exact/true solution of Eq. (16) is e^{t^3}, and the fitness/error function of above equation is given below:

Table 1 Workflow of optimization scheme GA-ASA in pseudocode

```
Genetic Algorithms procedure started
   Inputs: The chromosome/individual with equal number of unknown elements
      in the Networks as: W = [α, δ, β], where α = [α1, α2, α3, ..., αm],
      δ = [δ1, δ2, δ3, ..., δm] and β = [β1, β2, β3, ..., βm] .
      Population: A set of chromosomes represented as:
            P = [W1, W2, ,..., Wn]^t , wi = [αi, δi, βi]^t
   Output: The Best Global weights trained by GAs W_B.ga
   Initialization: Generate chromosome W with real bounded entries and
      initial population P with set of W vectors to make an initial P.
      Initialize parameters 'GA' and 'gaoptimset' routines.
   Fitness formulation: Obtain the fitness ε in P for all W using
equations (5) to (7).
   Termination: Terminate the procedure to attain any of the following
      •  'Fitness attained e → 10^-18'
      •  Tolerances '(TolFun and TolCon) → 10^-18', 'TolX →10^-20',
      •  'StallGenLimit →120', 'Generations→ 80'
      •  'PopulationSize → 300'
      •  Others taken as defaults of 'GA' functions.
      Go to step storage, when termination criteria meet,
   Ranking: Ranking is performed for each W of P as per their quality on
      fitness ε achieved.
   Reproduction:
      •  'Selection:@selectionuniform'.
      •  'Crossover:@crossoverheuristic'.
      •  'Mutations:@mutationadaptfeasible'.
      •  'Elitism: carry 5% individuals in next P,
      Go to 'fitness evaluation' step.
   Storage: Save the weight vector W_B.ga, fitness evaluation ε, time
      generation and function counts for the current run of GAs.
End Genetic algorithms
ASA Procedure Start
   Inputs: Start point: W_B.ga
   Output: GA-ASA best weights are denotes as W_GA.ASA
   Initialize: Set the bounded constraints, iterations and other
      parameters in 'optimset'.
   Terminate: ASA stops for any of the conditions meet: 'Fitness e ≤ 10^-16,
      Iterations = 1000, TolX ≤ 10^-20, (TolFun=TolCon) ≤ 10^-18 and
MaxFunEvals ≤ 220000.
   While (Required termination satisfied)
      Fitness evaluation: Calculate fitness value ε of each W of P by
using equations (5) to (7)
      Adjustments: Use 'fmincon' with 'active-set' method to tune W and
      Compute fitness value again by using equations (5) to (7).
      Accumulate: Store the values of weight vector W_GA.ASA, fitness ε,
time, number of generations and function counts for the said run of
ASA.
ASA Procedure End
Data Generations
      Repeat 100 times the GA-ASA process to get an enormous data-set of
the optimization variables of ANNs to solve third order singular model
```

$$\varepsilon = \frac{1}{N}\sum_{m=1}^{N}\left(t_m^2\hat{y}'''(t_m) + 4t_m\hat{y}''(t_m) + 2\hat{y}'(t_m)\right. \\ \left.-9t_m^2(4 + 10t_m^3 + 3t_m^6)\hat{y}\right)^2 \\ + \frac{1}{3}\left((\hat{y}_0 - 1)^2 + (\hat{y}'_0)^2 + (\hat{y}''_0)\right) \tag{17}$$

Case III Using $p = 3$ and $f(t)g(y) = -6(10 + 2t^3 + 6t^6)e^{-3y}$ in Eq. (1). The nonlinear Emden–Fowler equation takes the form as:

$$y'''(t) + \left(\frac{6}{t}\right)y''(t) + \left(\frac{6}{t^2}\right)y'(t) - 6(10 + 2t^3 + 6t^6)e^{-3y} = 0 \\ y(0) = 0,\ \ y'(0) = y''(0) = 0. \tag{18}$$

The exact/true solution of Eq. (18) is $\log(1 + t^3)$, and the fitness formulation of above case is written as:

$$\varepsilon = \frac{1}{N}\sum_{m=1}^{N}\left(t_m^2\hat{y}'''(t_m) + 6t_m\hat{y}''(t_m) + 6\hat{y}'(t_m)\right. \\ \left.-6t_m^2(10 + 2t_m^3 + 6t_m^6)e^{-3\hat{y}}\right)^2 \\ + \frac{1}{3}\left((\hat{y}_0)^2 + (\hat{y}'_0)^2 + (\hat{y}''_0)\right) \tag{19}$$

Case IV Take $p = 4$, $g(y) = y^m$ and $f(t) = 1$ in Eq. (1) using $m = 0$. The Lane–Emden Eq. (1) becomes in this case as:

$$y'''(t) + \left(\frac{8}{t}\right)y''(t) + \left(\frac{12}{t^2}\right)y'(t) + y^m = 0, \\ y(0) = 1,\ \ y'(0) = 0,\ \ y''(0) = 0. \tag{20}$$

The true solution of the model (20) is $1 - \frac{1}{90}t^3$, and error function becomes as:

$$\varepsilon = \frac{1}{N}\sum_{m=1}^{N}\left(t_m^2\hat{y}'''(t_m) + 8t_m\hat{y}''(t_m) + 12\hat{y}'(t_m) + t_m^2\hat{y}^m\right)^2 \\ + \frac{1}{3}\left((\hat{y}_0 - 1)^2 + (\hat{y}')^2 + (\hat{y}''_0)^2\right) \tag{21}$$

Case V By taking $p = 4$ and $g(y) = -(10 + 10t^3 + t^6)y$ in Eq. (1), the Emden–Fowler equation takes the form as

$$y'''(t) + \left(\frac{4}{t}\right)y''(t) - (t^6 + 10t^3 + 10)y = 0, \\ y(0) = 1,\ \ y'(0) = 0,\ \ y''(0) = 0. \tag{22}$$

The true solution of Eq. (23) is $e^{t^3}/3$, and error function becomes as:

$$\varepsilon = \frac{1}{N}\sum_{m=1}^{N}\left(t_m\hat{y}'''(t_m) + 4\hat{y}''(t_m) - t_m(10 + 10t_m^3 + t_m^6)^2\hat{y}\right. \\ \left. + \frac{1}{3}\left((\hat{y}_0 - 1)^2 + (\hat{y}'_0)^2 + (\hat{y}''_0)^2\right)\right. \tag{23}$$

Optimization is performed for all five cases of Emden–Fowler equation for the trained inputs between 0 and 1 with step 0.1 by the hybrid procedure GA-ASA for 100 independent trails. Optimized weights of ANNs for each case of the system are presented in Fig. 3, and these weights presented in Fig. 3a–e can be used in Eq. 4 to find the approximate results of proposed ANN–GA–ASA in the trained interval [0, 1] for solving cases 1, 2, 3, 4 and 5 of the nonlinear singular Emden–Fowler system (1), respectively. The solutions of proposed ANN–GA–ASA are determined using weight in Fig. 3 in (4) for both trained input grid, i.e., [0. 0.1, 0.2, …, 1] and testing input grid [0.05, 0.15, …, 0.95], and results are illustrated in Fig. 4a–d, f along with the reference exact solutions for cases 1, 2, 3, 4 and 5 of Emden–Fowler system (1), respectively.

The results of ANN–GA–ASA are consistently overlapping with exact solution for both training and testing points for each case of the system. In order to show the level of precision achieved, the values of absolute error (AE) from reference exact solutions are determined for both training and testing input grids and results are presented in Fig. 5 on semi-logarithmic scale. The absolute error plots are shown in Fig. 5a–d, e of proposed ANN–GA–ASA for nonlinear third-order Emden–Fowler equation for all respective five cases. The value of AE lies in the range 10^{-09}–10^{-06}, 10^{-06}–10^{-04}, 10^{-05}–10^{-07}, 10^{-09}–10^{-07} and 10^{-06}–10^{-09} for both train and test points of cases 1, 2, 3, 4 and 5, respectively. No noticeable difference exists between training and testing results established the worth of the ANN–GA–ASA for solving Emden–Fowler equation.

Hundred trials of ANN–GA–ASA are conducted for finding the solution of Emden–Fowler Eq. (1) for all five cases. The best solutions with minimum value of error-based fitness, mean solutions and reference exact results are plotted in Fig. 6 for all five cases of model (1). It is clear from all five Fig. 6a–e that the best and mean solutions are overlapped with the true solutions for all cases. The comparison of the performance is conducted on the basis of best, worst and mean values of the absolute error from all 100 independent executions of proposed ANN–GA–ASA, and results are presented in Fig. 7 which have five subfigures and Table 2 for all five variations of Emden–Fowler system (1).

Additionally, the values of performances metrics MAD, TIC and ENSE are calculated for best, worst and mean

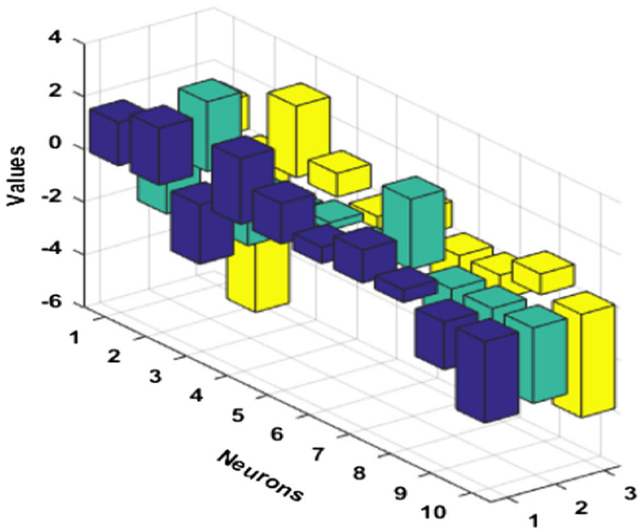

(a) ANNs weights for Case 1

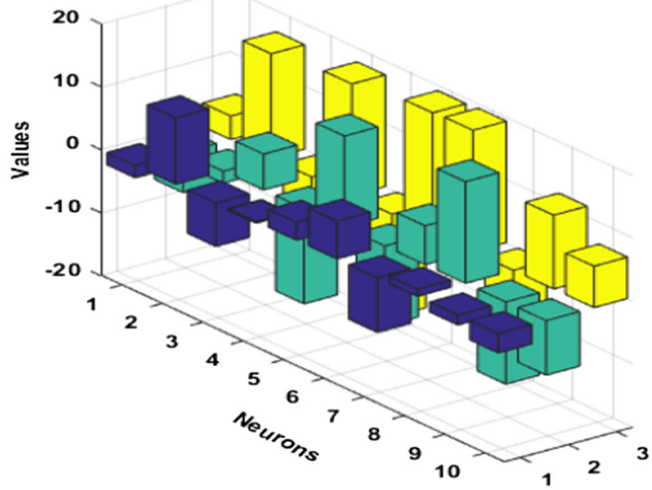

(b) ANNs weights for Case 2

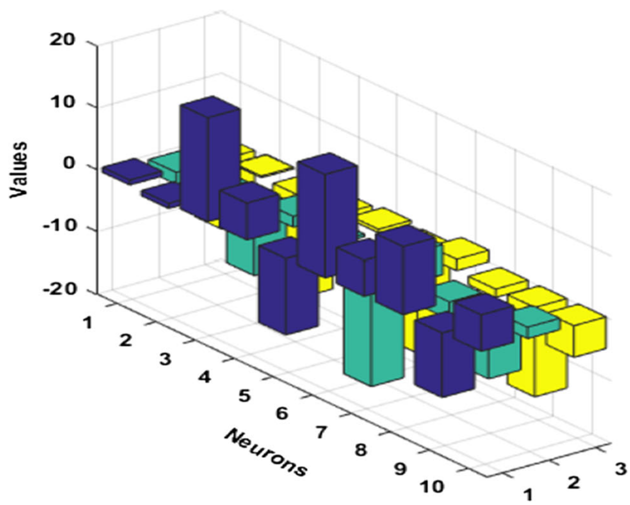

(c) ANNs weights for Case 3

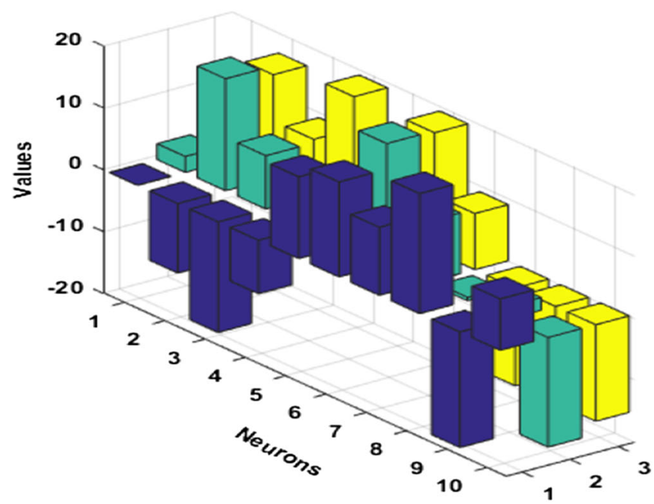

(d) ANNs weights for Case 4

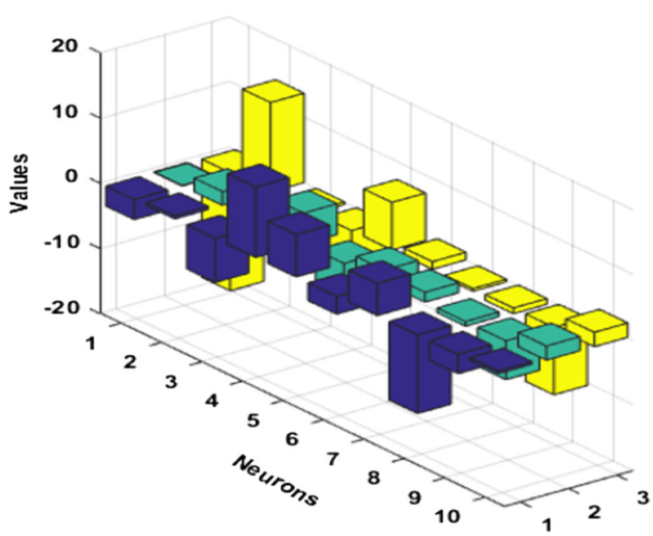

(e) ANNs weights for Case 5

Fig. 3 Set of weights by proposed ANN–GA–ASA for nonlinear third-order Emden–Fowler equation for all cases

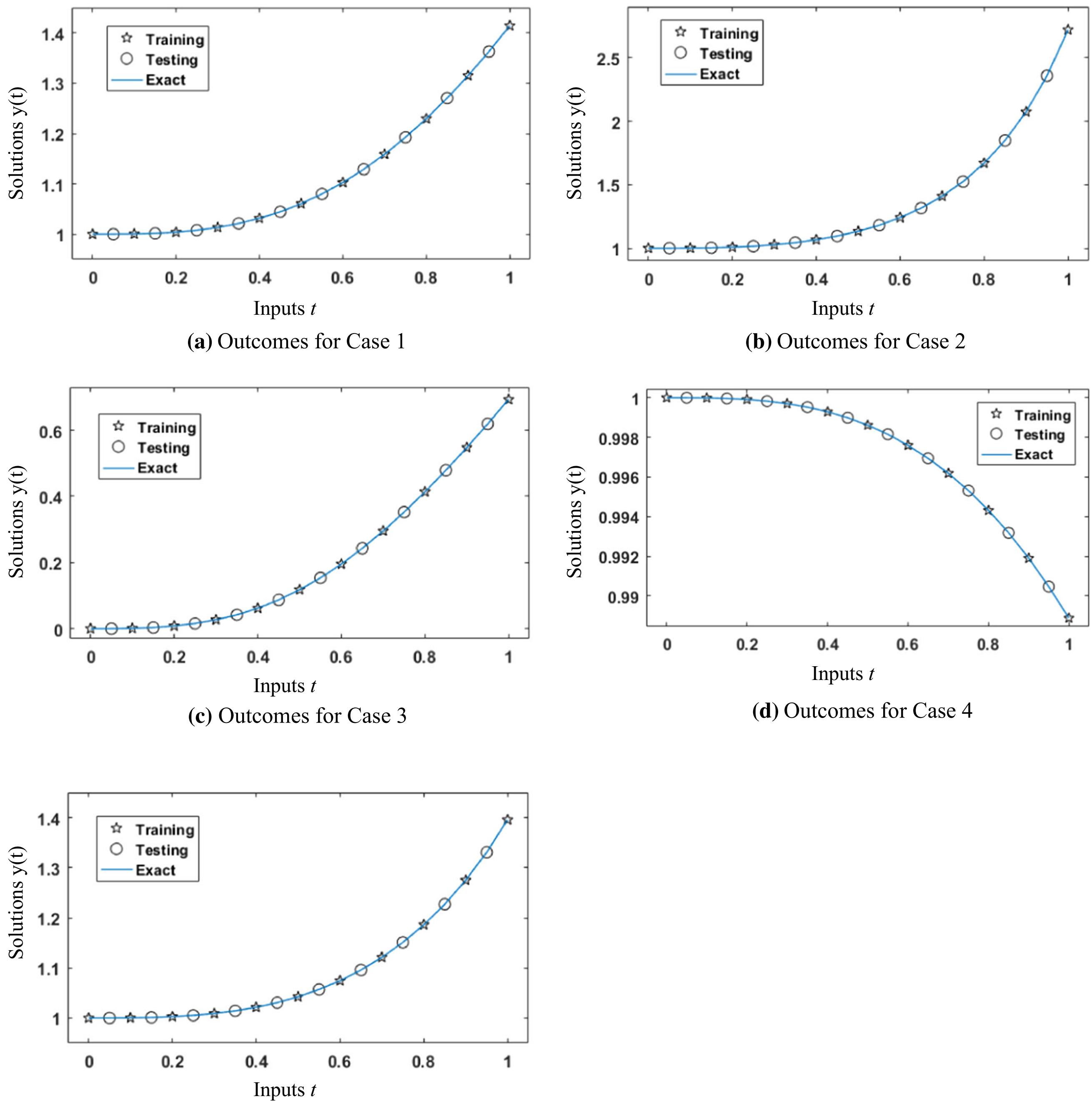

(a) Outcomes for Case 1
(b) Outcomes for Case 2
(c) Outcomes for Case 3
(d) Outcomes for Case 4
(e) Outcomes for Case 5

Fig. 4 Comparison of results for training and testing of proposed ANN–GA–ASA with exact solution for nonlinear third-order Emden–Fowler equation for all five cases

values of the absolute error from all 100 independent executions of proposed ANN–GA–ASA and results are presented in Fig. 8 for all five variations of nonlinear third-order Emden–Fowler model.

One may observe from results presented in Fig. 7 and Table 3 that the values of AE lie around 10^{-06}–10^{-07}, 10^{-04}–10^{-05}, 10^{-06}–10^{-08}, 10^{-06}–$10^{-09}$and 10^{-07}–10^{-09} for the best solutions for cases 1–5, respectively, while respective average values are 10^{-02}–10^{-03}, 10^{-01}–10^{-02}, 10^{-02}–10^{-03}, 10^{-02}–10^{-04} and 10^{-04} to 10^{-05}. The statistical analysis presented in the terms of minimum (Min), mean (Mean) and standard deviation (SD) in Table 2 shows that Min values lie in the ranges of [10^{-07}, 10^{-08}] for case 1, [10^{-05}, 10^{-06}] for case 2, [10^{-06}, 10^{-08}] for case 3, [10^{-08}, 10^{-10}] for case 4 and [10^{-07}, 10^{-09}] for case 5, whereas the mean values mostly lie in the ranges of

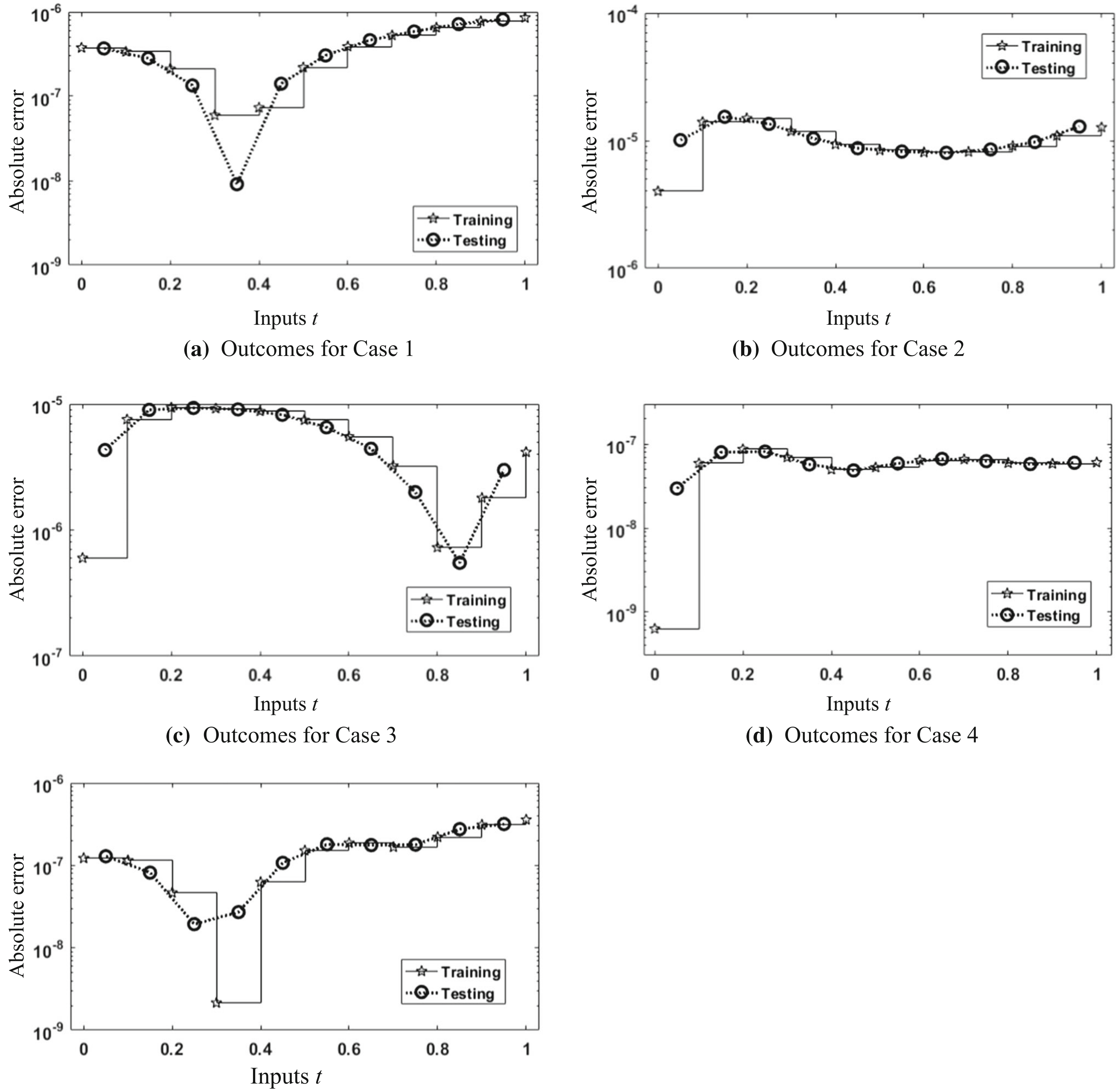

(a) Outcomes for Case 1 **(b)** Outcomes for Case 2

(c) Outcomes for Case 3 **(d)** Outcomes for Case 4

(e) Outcomes for Case 5

Fig. 5 Comparison of results for training and testing of proposed ANN–GA–ASA for nonlinear third-order Emden–Fowler equation for all five cases

[10^{-02}, 10^{-03}] but in some cases range [10^{-05}, 10^{-06}] as well. Moreover, the SD values in small ranges for all the cases. These results further endorsed the consistent reasonable precision of all three performance metrics MAD, TIC and ENSE for proposed ANN–GA–ASA.

Analysis on the performance of ANN–GA–ASA is further examined on the basis of histograms studies. The values of the fitness, MAD, TIC and ENSE are illustrated graphically in Figs. 9, 10, 11 and 12, respectively. The presented results show that respective MAD, TIC and ENSE values for cases 1–5 lie around 10^{-06}–10^{-08}, 10^{-04}–10^{-06}, 10^{-04}–10^{-06}, 10^{-06}–10^{-08} and 10^{-05}–10^{-07}, 10^{-10}–10^{-12}, 10^{-08}–10^{-10}, 10^{-08}–10^{-09}, 10^{-11}–10^{-12} and 10^{-12}–10^{-14}, 10^{-09}–10^{-10}, 10^{-09}–10^{-10}, 10^{-11}–10^{-12} and 10^{-13}–10^{-15}. The mean values of MAD lie around 10^{-02}–10^{-04}, 10^{-02}–10^{-04}, 10^{-02}–10^{-03}, 10^{-02}–10^{-04} and 10^{-01}–10^{-03}. The histogram plotted for all four performances measure show the consistence of the convergence

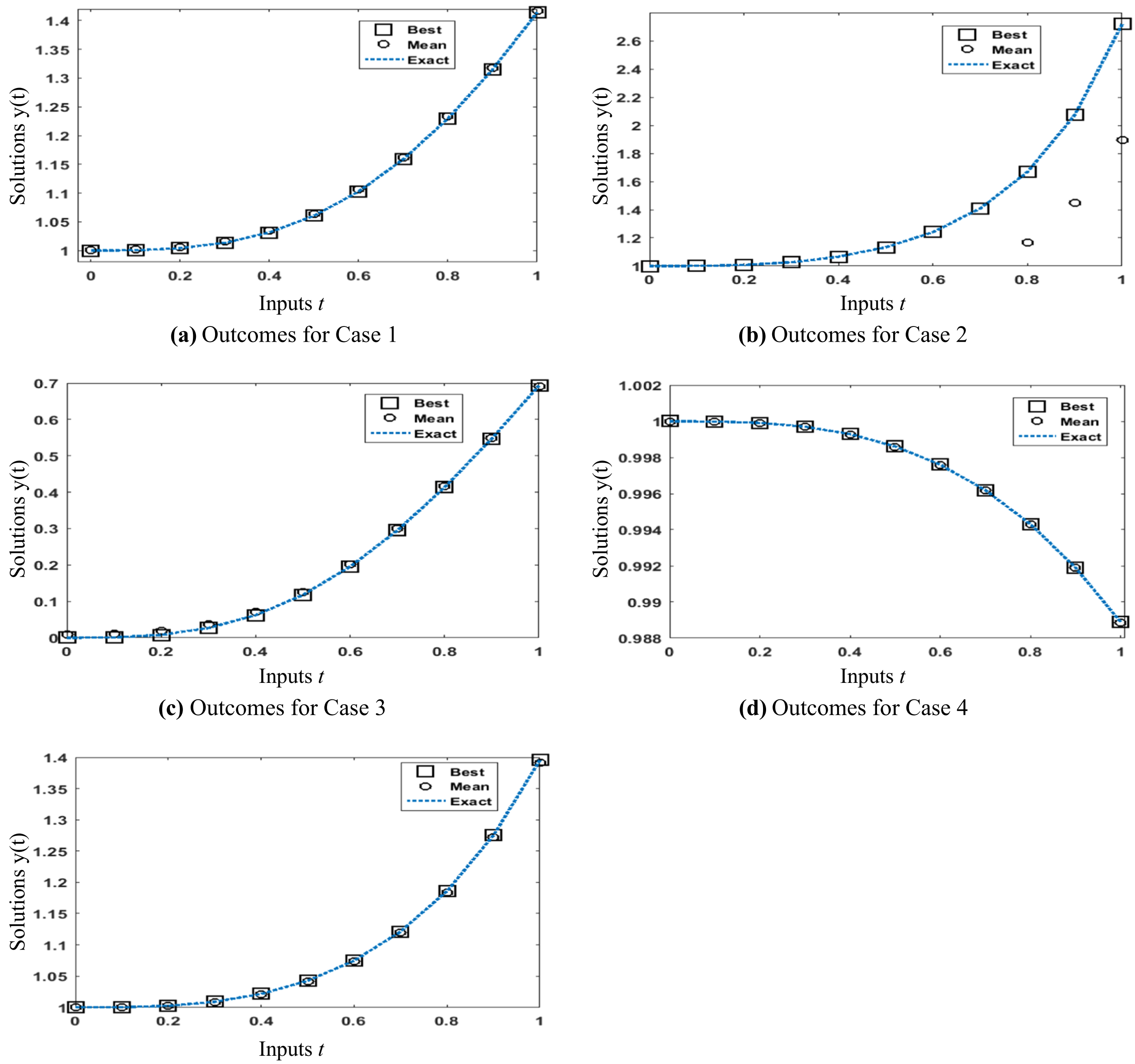

(a) Outcomes for Case 1

(b) Outcomes for Case 2

(c) Outcomes for Case 3

(d) Outcomes for Case 4

(e) Outcomes for Case 5

Fig. 6 The best and mean values of approximate solutions of proposed ANN–GA–ASA and their comparison with exact results for all five cases

and the precision of ANN-GA-AS on the basis of fitness, TIC, MAD and ENSE.

The results of global performance operators, i.e., GFIT, GMAD, GTIC and GENSE being the average values of fitness, MAD, TIC and ENSE, for 100 executions of ANN–GA–ASA are tabulated in Table 3 for all five cases of third-order nonlinear Emden–Fowler model. The magnitude (Mag) and SD of these global operators show reasonable precision for all four global statistical operators [GFIT, GMAD, GTIC and GENSE] for each scenario of the problem.

5 Conclusion

The motivation behind this study is to solve third-order nonlinear singular differential model by exploiting the strength of integrated intelligent computing paradigm based on artificial neural network models optimized with genetic algorithm hybrid with active-set technique. Some of the key findings are summarized below

- Artificial neural network is successfully applied to solve the third-order nonlinear singular differential model.

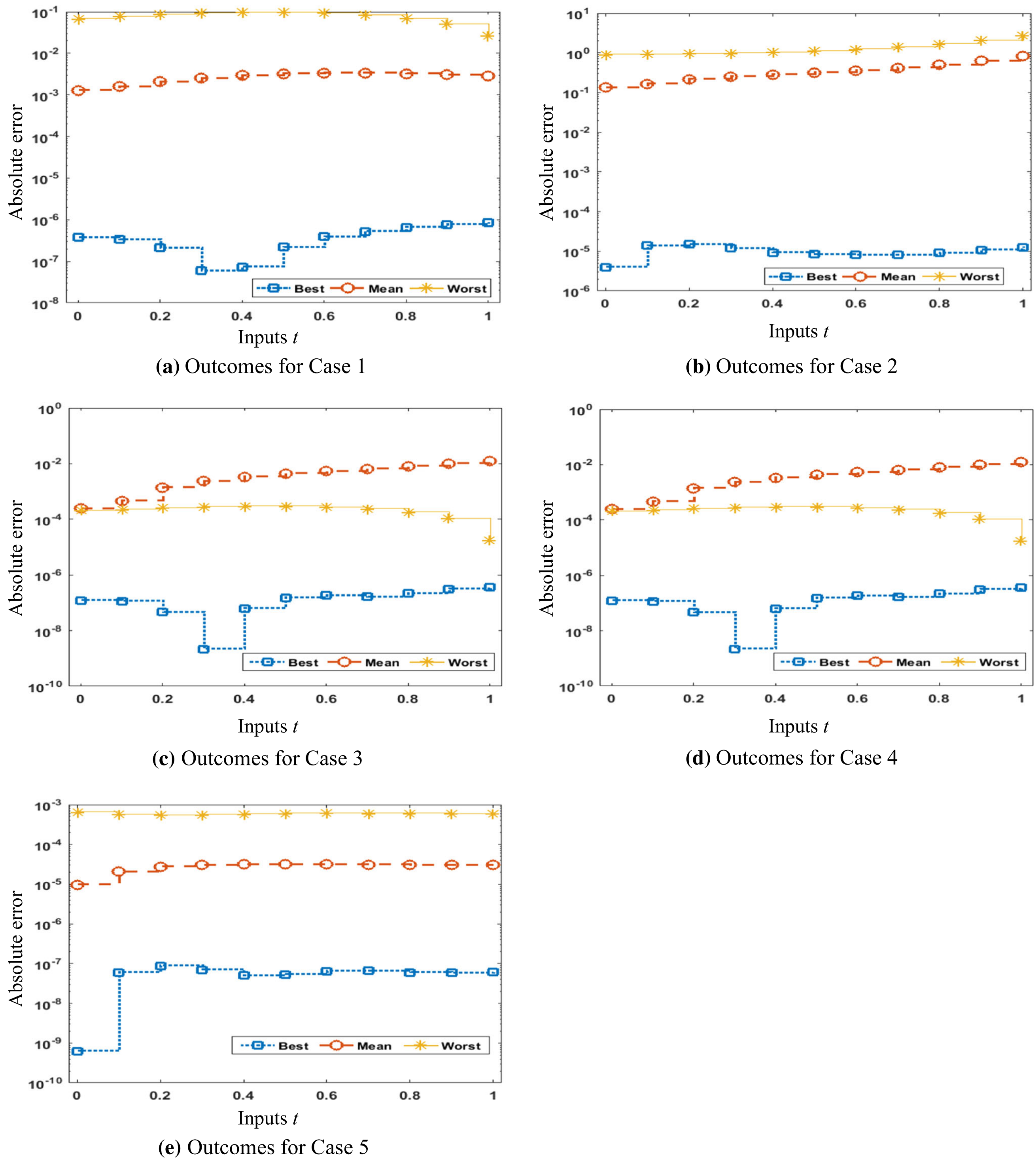

Fig. 7 The best, mean and worst values of absolute error for the proposed ANN–GA–ASA for all five cases

- The accuracy and convergence of the present method are analyzed through the outcomes of statistical measures based on 100 independent runs to solve five cases of third-order nonlinear singular differential model.
- The best AE values lie up to 10^{-05}–10^{-09}. However, the worst solution of AE also lies up to 10^{-01}–10^{-05}.
- The global FIT, MAD, TIC and ENSE are presented with good agreements with their optimal gauges.

The presented scheme ANN–GA–ASA looks promising to be exploited for solving the higher order nonlinear

Table 2 Statistics results for all cases of singular model

x	Case 1			Case 2			Case 3			Case 4			Case 5		
	Min	Max	STD	Min	Max	STD	Min	Max	STD	Min	Max	STD	Min	Max	STD
0	3.2E−08	1.3E−03	6.8E−03	4.0E−06	1.3E−01	2.8E−01	1.7E−07	1.0E−02	5.3E−02	1.5E−10	9.6E−06	6.6E−05	6.6E−08	2.4E−04	1.5E−03
0.1	1.1E−08	1.6E−03	7.8E−03	1.4E−05	1.7E−01	2.9E−01	2.6E−07	1.0E−02	5.4E−02	2.9E−08	2.1E−05	6.3E−05	1.1E−07	4.6E−04	3.1E−03
0.2	2.1E−07	2.1E−03	9.3E−03	9.0E−06	2.2E−01	3.4E−01	9.3E−06	1.1E−02	5.4E−02	7.9E−08	2.7E−05	7.5E−05	4.7E−08	1.4E−03	9.2E−03
0.3	6.0E−08	2.5E−03	1.1E−02	3.6E−06	2.5E−01	3.8E−01	9.2E−06	1.0E−02	5.3E−02	6.7E−08	3.0E−05	9.0E−05	2.1E−09	2.4E−03	1.5E−02
0.4	5.1E−08	2.9E−03	1.3E−02	2.1E−06	2.9E−01	4.2E−01	8.7E−06	9.6E−03	5.0E−02	5.0E−08	3.1E−05	1.0E−04	1.7E−08	3.3E−03	2.1E−02
0.5	2.2E−07	3.2E−03	1.4E−02	1.5E−06	3.2E−01	4.7E−01	7.4E−06	8.5E−03	4.6E−02	5.3E−08	3.2E−05	1.1E−04	8.5E−08	4.4E−03	2.8E−02
0.6	2.7E−07	3.4E−03	1.5E−02	8.1E−06	3.6E−01	5.3E−01	5.5E−06	7.0E−03	3.9E−02	6.5E−08	3.1E−05	1.1E−04	2.5E−08	5.4E−03	3.4E−02
0.7	3.7E−07	3.4E−03	1.6E−02	4.7E−06	4.2E−01	6.2E−01	3.1E−06	5.0E−03	3.0E−02	6.6E−08	3.1E−05	1.1E−04	2.0E−08	6.5E−03	4.1E−02
0.8	2.3E−07	3.2E−03	1.6E−02	9.1E−06	5.0E−01	7.4E−01	4.1E−08	2.9E−03	2.0E−02	3.6E−08	3.0E−05	1.0E−04	7.8E−08	8.2E−03	5.3E−02
0.9	1.3E−08	3.0E−03	1.6E−02	1.1E−05	6.3E−01	9.3E−01	9.2E−07	1.6E−03	1.0E−02	5.9E−08	3.0E−05	1.0E−04	7.6E−08	1.0E−02	6.7E−02
1	2.3E−07	2.9E−03	1.5E−02	1.3E−05	8.2E−01	1.2E+00	4.1E−06	1.8E−03	6.4E−03	3.0E−08	3.0E−05	1.0E−04	2.8E−07	1.2E−02	8.3E−02

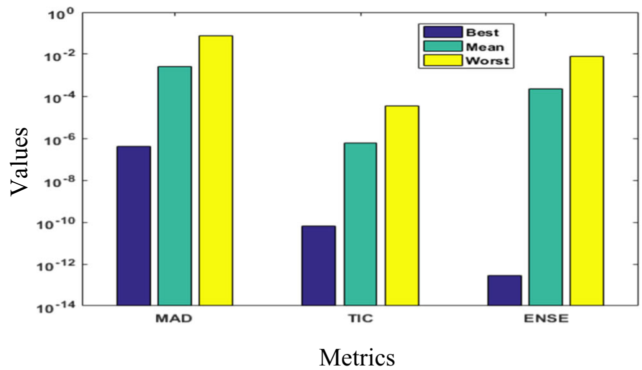

(a) Outcomes for Case 1

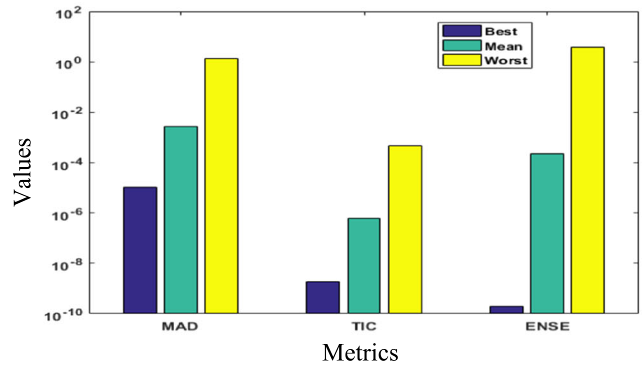

(b) Outcomes for Case 2

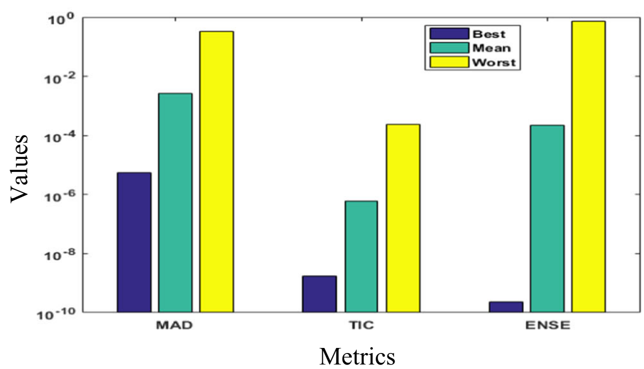

(c) Outcomes for Case 3

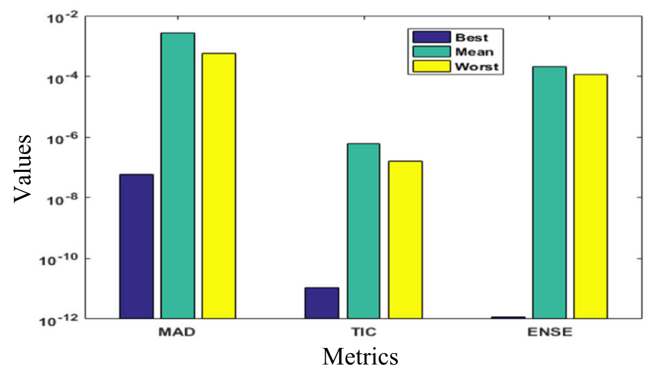

(d) Outcomes for Case 4

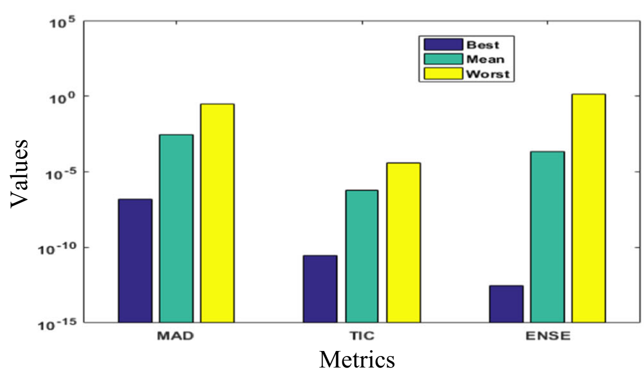

(e) Outcomes for Case 5

Fig. 8 The MAD, TIC and ENSE values of the performance indices for the proposed ANN–GA–ASA for all five cases

Table 3 Global performance results for all five cases

Index	Cases	GFIT		GMAD		GTIC		GENSE	
		Mag	S.D	Mag	S.D	Mag	S.D	Mag	S.D
$\hat{y}(x)$	1	9.4E−05	6.6E−04	2.7E−03	1.2E−02	6.1E−07	3.6E−06	2.2E−04	1.2E−03
	2	4.2E−02	9.2E−02	3.7E−01	5.5E−01	5.2E−05	8.9E−05	1.0E+00	1.6E+00
	3	2.0E−03	1.3E−02	7.1E−03	3.7E−02	2.8E−06	2.3E−05	1.1E−02	7.8E−02
	4	3.7E−06	1.6E−05	2.8E−05	9.0E−05	4.3E−09	1.7E−08	3.2E−06	1.7E−05
	5	7.5E−05	4.8E−04	5.0E−03	3.2E−02	5.9E−07	3.9E−06	1.5E−02	1.4E−01

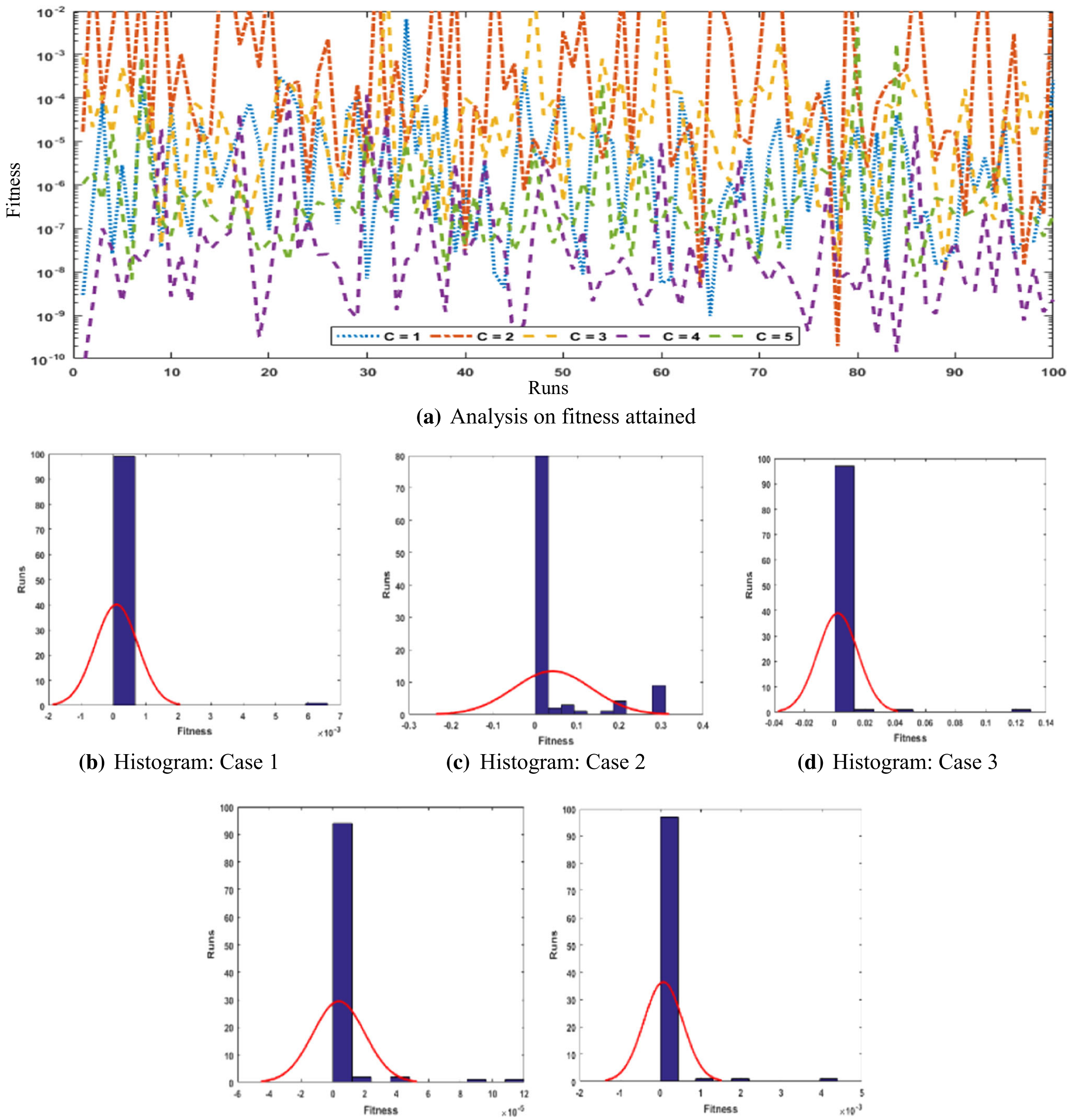

(a) Analysis on fitness attained

(b) Histogram: Case 1

(c) Histogram: Case 2

(d) Histogram: Case 3

(e) Histogram: Case 2

(f) Histogram: Case 3

Fig. 9 The comparison on fitness through histogram studies for the proposed ANN–GA–ASA for all five cases

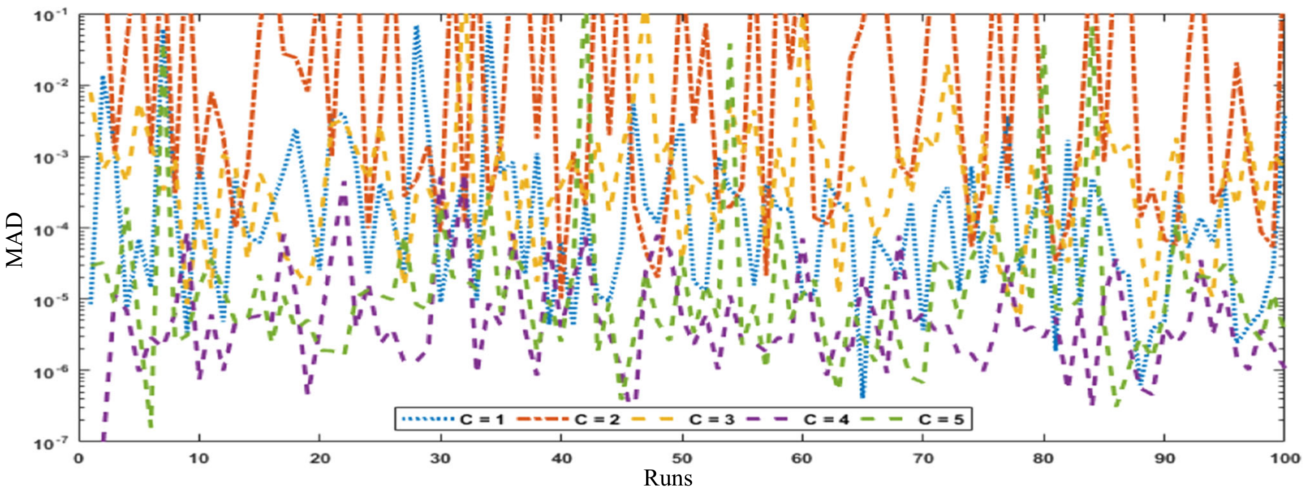

(a) Analysis on MAD values

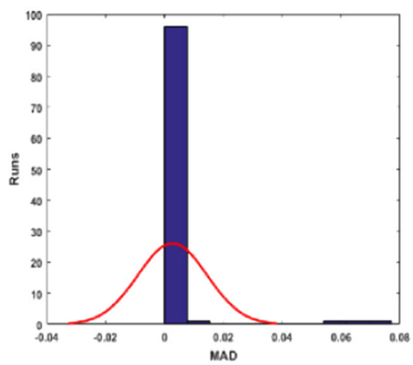

(b) Histogram: Case 1

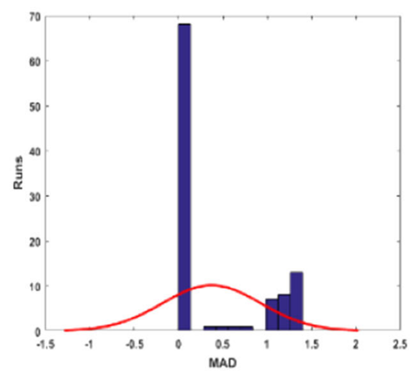

(c) Histogram: Case 2

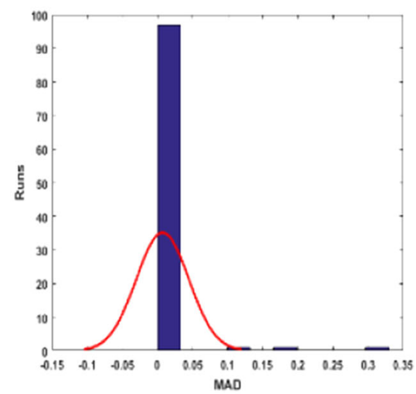

(d) Histogram: Case 3

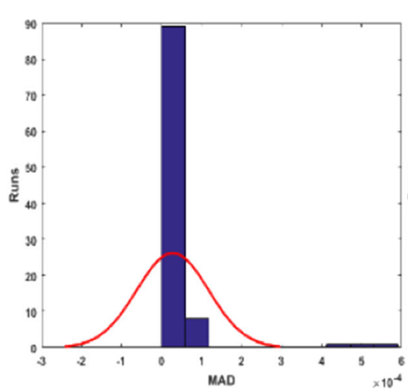

(e) Histogram: Case 2

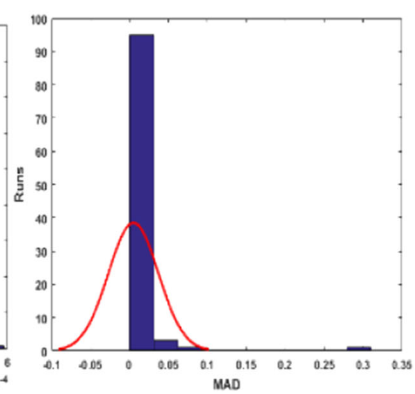

(f) Histogram: Case 3

Fig. 10 The comparison on MAD values through histogram studies for the proposed ANN–GA–ASA for all five cases

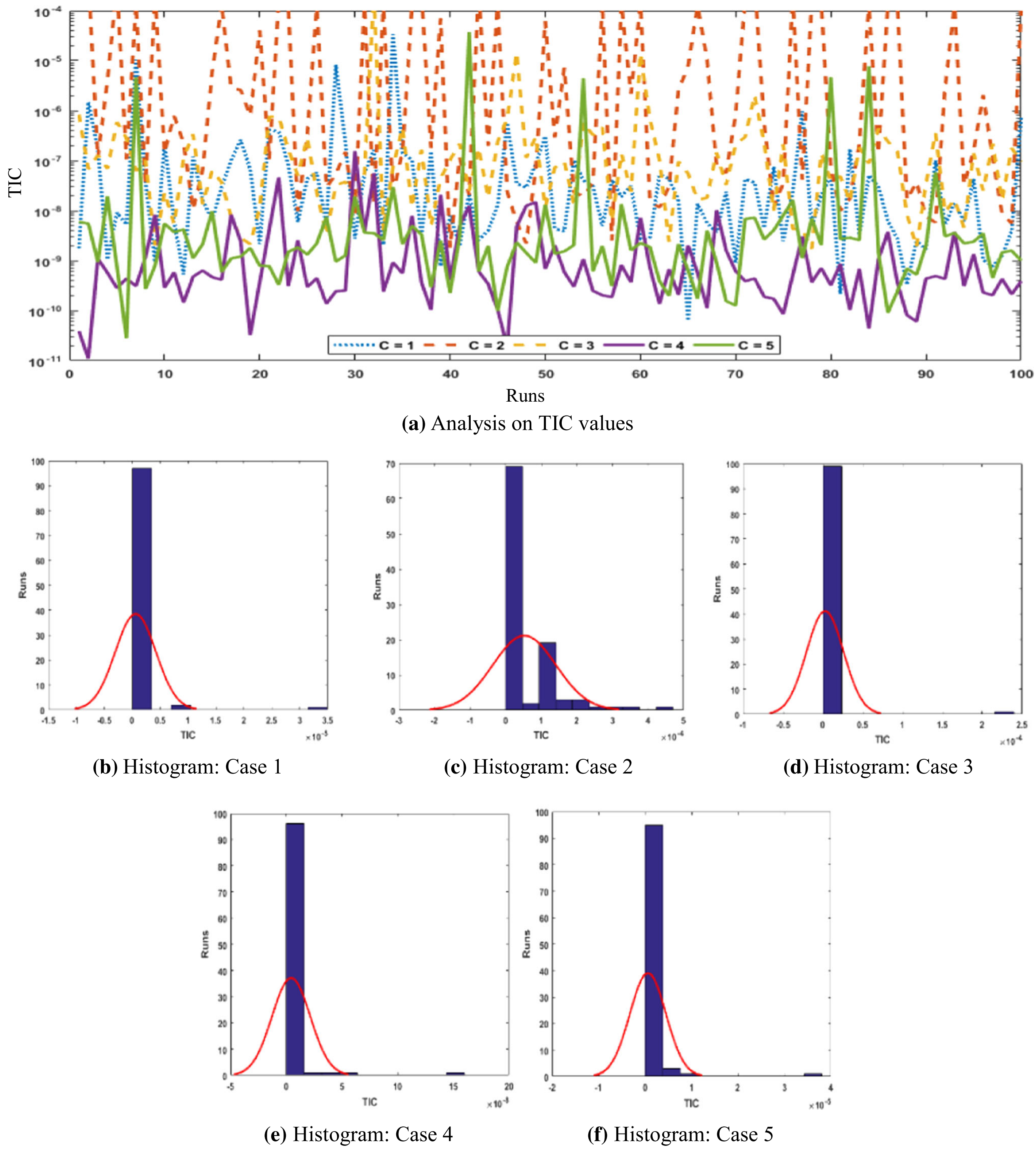

Fig. 11 The comparison on TIC values through histogram studies for the proposed ANN–GA–ASA for all five cases

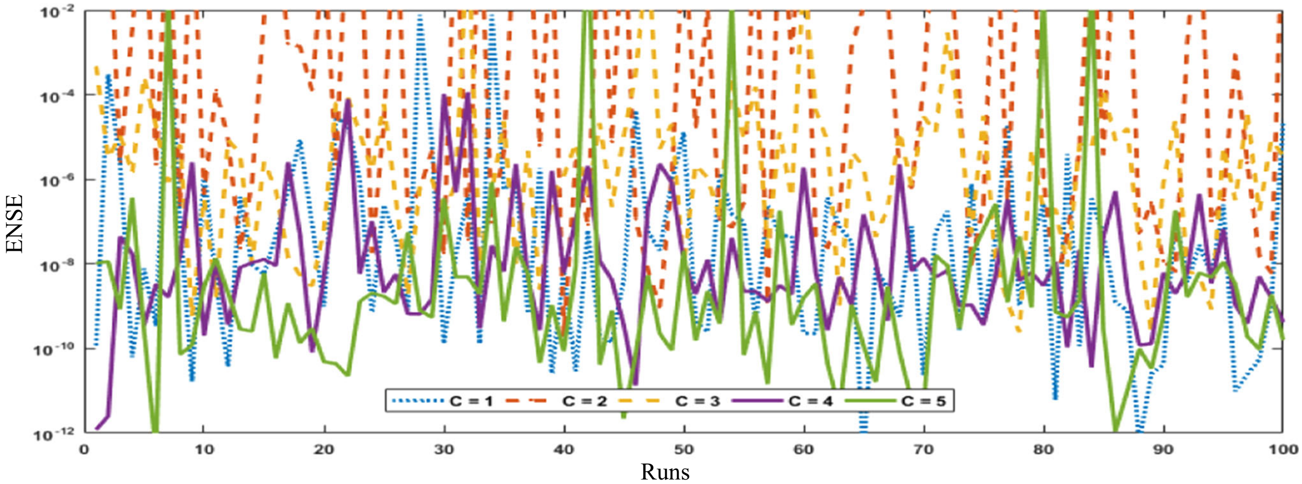

(a) Analysis on TIC values

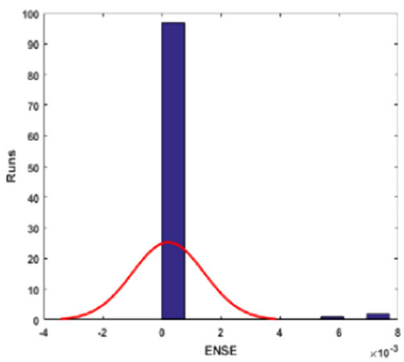

(b) Histogram: Case 1

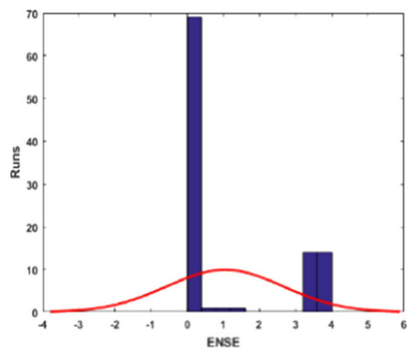

(c) Histogram: Case 2

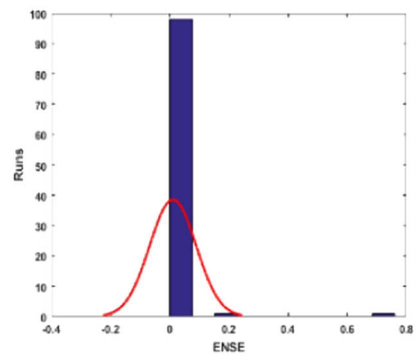

(d) Histogram: Case 3

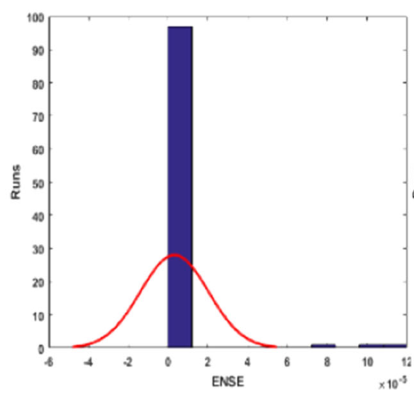

(e) Histogram: Case 4

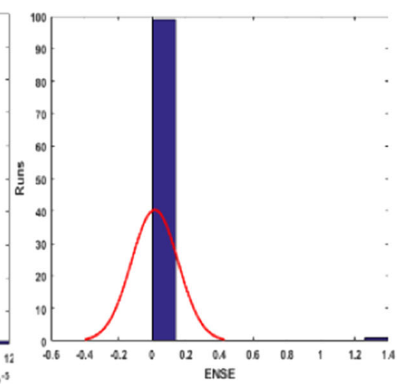

(f) Histogram: Case 5

Fig. 12 The comparison on ENSE values through histogram studies for the proposed ANN–GA–ASA for all five cases singular systems represented with differential equations involving both integer and fractional order derivatives.

References

1. Lane HJ (1870) On the theoretical temperature of the sun, under the hypothesis of a gaseous mass maintaining its volume by its internal heat and depending on the laws of gases as known to terrestrial experiment. Am J Sci 148:57–74
2. Emden R (1907) Gaskugeln Teubner. Leipzig und Berlin
3. Ahmad I et al (2017) Neural network methods to solve the Lane–Emden type equations arising in thermodynamic studies of the spherical gas cloud model. Neural Comput Appl 28(1):929–944
4. Baleanu D, Sajjadi SS, Jajarmi A, Asad JH (2019) New features of the fractional Euler–Lagrange equations for a physical system within non-singular derivative operator. Eur Phys J Plus 134(4):181
5. Luo T, Xin Z, Zeng H (2016) Nonlinear asymptotic stability of the Lane–Emden solutions for the viscous gaseous star problem with degenerate density dependent viscosities. Commun Math Phys 347(3):657–702
6. Rach R, Duan JS, Wazwaz AM (2014) Solving coupled Lane–Emden boundary value problems in catalytic diffusion reactions by the Adomian decomposition method. J Math Chem 52(1):255–267
7. Boubaker K, Van Gorder RA (2012) Application of the BPES to Lane–Emden equations governing polytropic and isothermal gas spheres. New Astron 17(6):565–569
8. Taghavi A, Pearce S (2013) A solution to the Lane–Emden equation in the theory of stellar structure utilizing the Tau method. Math Methods Appl Sci 36(10):1240–1247
9. Khan JA et al (2015) Nature-inspired computing approach for solving non-linear singular Emden-Fowler problem arising in electromagnetic theory. Connect Sci 27(4):377–396
10. Bhrawy AH, Alofi AS, Van Gorder RA (2014) An efficient collocation method for a class of boundary value problems arising in mathematical physics and geometry. In: Abstract and Applied Analysis, vol 2014. Hindawi Publishing Corporation
11. Ramos JI (2003) Linearization methods in classical and quantum mechanics. Comput Phys Commun 153(2):199–208
12. Dehghan M, Shakeri F (2008) Solution of an integro-differential equation arising in oscillating magnetic fields using He's homotopy perturbation method. Prog Electromagn Res 78:361–376
13. Radulescu V, Repovs D (2012) Combined effects in nonlinear problems arising in the study of anisotropic continuous media. Nonlinear Anal Theory Methods Appl 75(3):1524–1530
14. Flockerzi D, Sundmacher K (2011) On coupled Lane–Emden equations arising in dusty fluid models. In: Journal of Physics: Conference Series, vol 268, no 1. IOP Publishing, p 012006
15. Ghergu M, Radulescu V (2007) On a class of singular Gierer-Meinhardt systems arising in morphogenesis. Comptes Rendus Mathématique 344(3):163–168
16. Wazwaz AM (2015) Solving two Emden–Fowler type equations of third order by the variational iteration method. Appl Math Inf Sci 9(5):2429
17. Shawagfeh NT (1993) Non perturbative approximate solution for Lane–Emden equation. J Math Phys 34(9):4364–4369
18. Wazwaz AM (2001) A new algorithm for solving differential equations of Lane–Emden type. Appl Math Comput 118(2):287–310
19. Liao S (2003) A new analytic algorithm of Lane–Emden type equations. Appl Math Comput 142(1):1–16
20. He JH, Ji FY (2019) Taylor series solution for Lane–Emden equation. J Math Chem 57(8):1932–1934
21. Nouh MI (2004) Accelerated power series solution of polytropic and isothermal gas spheres. New Astron 9(6):467–473
22. Mandelzweig VB, Tabakin F (2001) Quasilinearization approach to nonlinear problems in physics with application to nonlinear ODEs. Comput Phys Commun 141(2):268–281
23. Ahmad I et al (2019) Novel applications of intelligent computing paradigms for the analysis of nonlinear reactive transport model of the fluid in soft tissues and microvessels. Neural Comput Appl 31(12):9041–9059
24. Fateh MF et al (2019) Differential evolution based computation intelligence solver for elliptic partial differential equations. Front Inf Technol Electron Eng 20(10):1445–1456
25. Ahmad I et al (2019) Design of computational intelligent procedure for thermal analysis of porous fin model. Chin J Phys 59:641–655
26. Raja MAZ et al (2016) A new numerical approach to solve Thomas-Fermi model of an atom using bio-inspired heuristics integrated with sequential quadratic programming. Springer Plus 5(1):1400
27. Umar M et al (2019) Intelligent computing for numerical treatment of nonlinear prey–predator models. Appl Soft Comput 80:506–524
28. Raja MAZ, Shah FH, Tariq M, Ahmad I (2018) Design of artificial neural network models optimized with sequential quadratic programming to study the dynamics of nonlinear Troesch's problem arising in plasma physics. Neural Comput Appl 29(6):83–109
29. Jafarian A, Mokhtarpour M, Baleanu D (2017) Artificial neural network approach for a class of fractional ordinary differential equation. Neural Comput Appl 28(4):765–773
30. Raja MAZ, Shah FH, Alaidarous ES, Syam MI (2017) Design of bio-inspired heuristic technique integrated with interior-point algorithm to analyze the dynamics of heartbeat model. Appl Soft Comput 52:605–629
31. Ghehsareh HR, Zaghian A, Zabetzadeh SM (2018) The use of local radial point interpolation method for solving two-dimensional linear fractional cable equation. Neural Comput Appl 29(10):745–754
32. Raja MAZ, Niazi SA, Butt SA (2017) An intelligent computing technique to analyze the vibrational dynamics of rotating electrical machine. Neurocomputing 219:280–299
33. He W, Chen Y, Yin Z (2016) Adaptive neural network control of an uncertain robot with full-state constraints. IEEE Trans Cybern 46(3):620–629
34. Schaff JC, Gao F, Li Y, Novak IL, Slepchenko BM (2016) Numerical approach to spatial deterministic-stochastic models arising in cell biology. PLoS Comput Biol 12(12):e1005236
35. Pelletier F, Masson C, Tahan A (2016) Wind turbine power curve modelling using artificial neural network. Renew Energy 89:207–214
36. Zameer A et al (2017) Intelligent and robust prediction of short term wind power using genetic programming based ensemble of neural networks. Energy Convers Manag 134:361–372
37. Zúñiga-Aguilar CJ, Coronel-Escamilla A, Gómez-Aguilar JF, Alvarado-Martínez VM, Romero-Ugalde HM (2018) New numerical approximation for solving fractional delay differential equations of variable order using artificial neural networks. Eur Phys J Plus 133(2):75
38. Rizaner FB, Rizaner A (2018) Approximate solutions of initial value problems for ordinary differential equations using radial basis function networks. Neural Process Lett 48(2):1063–1071
39. Ghasemi S, Nazemi A (2019) A fractional power series neural network for solving a class of fractional optimal control problems

with equality and inequality constraints. Netw Comput Neural Syst 30(1–4):148–175
40. Holland JH (1992) Genetic algorithms. Sci Am 267(1):66–73
41. Srinivas N, Deb K (1994) Muilti-objective optimization using no dominated sorting in genetic algorithms. Evol Comput 2(3):221–248
42. Mehmood A et al (2019) Integrated computational intelligent paradigm for nonlinear electric circuit models using neural networks, genetic algorithms and sequential quadratic programming. Neural Comput Appl. https://doi.org/10.1007/s00521-019-04573-3
43. Chang FS, Wu JS, Lee CN, Shen HC (2014) Greedy-search-based multi-objective genetic algorithm for emergency logistics scheduling. Expert Syst Appl 41(6):2947–2956
44. Majeed K et al (2017) A genetic algorithm optimized Morlet wavelet artificial neural network to study the dynamics of nonlinear Troesch's system. Appl Soft Comput 56:420–435
45. Vaishnav P, Choudhary N, Jain K (2017) Traveling salesman problem using genetic algorithm: a survey. Int J Sci Res Comput Sci Eng Inf Technol 2(3):105–108
46. Raja MAZ, Shah AA, Mehmood A, Chaudhary NI, Aslam MS (2018) Bio-inspired computational heuristics for parameter estimation of nonlinear Hammerstein controlled autoregressive system. Neural Comput Appl 29(12):1455–1474
47. Duvvuri SP, Anmala J (2019) Fecal coliform predictive model using genetic algorithm-based radial basis function neural networks (GA-RBFNNs). Neural Comput Appl 31(12):8393–8409
48. Mehmood A et al (2018) Design of neuro-computing paradigms for nonlinear nanofluidic systems of MHD Jeffery-Hamel flow. J Taiwan Inst Chem Eng 91:57–85
49. Baroudi U, Bin-Yahya M, Alshammari M, Yaqoub U (2019) Ticket-based QoS routing optimization using genetic algorithm for WSN applications in smart grid. J Ambient Intell Humaniz Comput 10(4):1325–1338
50. Mehmood A et al (2019) Integrated intelligent computing paradigm for the dynamics of micropolar fluid flow with heat transfer in a permeable walled channel. Appl Soft Comput 79:139–162
51. Neysiani BS, Soltani N, Mofidi R, Nadimi-Shahraki MH (2019) Improve performance of association rule-based collaborative filtering recommendation systems using genetic algorithm. Int J Inf Technol Comput Sci 2:48–55
52. Ahmadi MH, Ahmadi MA, Nazari MA, Mahian O, Ghasempour R (2019) A proposed model to predict thermal conductivity ratio of Al_2O_3/EG nanofluid by applying least squares support vector machine (LSSVM) and genetic algorithm as a connectionist approach. J Therm Anal Calorim 135(1):271–281
53. Deuerlein JW, Piller O, Elhay S, Simpson AR (2019) Content-based active-set method for the pressure-dependent model of water distribution systems. J Water Resour Plan Manag 145(1):04018082
54. Azizi M, Amirfakhrian M, Araghi MAF (2019) A fuzzy system based active set algorithm for the numerical solution of the optimal control problem governed by partial differential equation. Eur J Control 54:99–110
55. Koehler S, Danielson C, Borrelli F (2017) A primal-dual active-set method for distributed model predictive control. Optimal Control Appl Methods 38(3):399–419
56. Wang X, Pardalos PM (2017) A modified active set algorithm for transportation discrete network design bi-level problem. J Glob Optim 67(1–2):325–342
57. Shen C, Zhang LH, Yang WH (2016) A filter active-set algorithm for ball/sphere constrained optimization problem. SIAM J Optim 26(3):1429–1464
58. Stam CJ, Reijneveld JC (2007) Graph theoretical analysis of complex networks in the brain. Nonlinear Biomed Phys 1(1):3
59. Bullmore E, Sporns O (2009) Complex brain networks: graph theoretical analysis of structural and functional systems. Nat Rev Neurosci 10(3):186–198
60. Cao J, Xiao M (2007) Stability and Hopf bifurcation in a simplified BAM neural network with two time delays. IEEE Trans Neural Netw 18(2):416–430
61. Raja MAZ, Khan JA, Zameer A, Khan NA, Manzar MA (2019) Numerical treatment of nonlinear singular Flierl-Petviashivili systems using neural networks models. Neural Comput Appl 31:2371–2394
62. Munir A, Manzar MA, Khan NA, Raja MAZ (2019) Intelligent computing approach to analyze the dynamics of wire coating with Oldroyd 8-constant fluid. Neural Comput Appl 31(3):751–775
63. Raja MAZ, Mehmood J, Sabir Z, Nasab AK, Manzar MA (2019) Numerical solution of doubly singular nonlinear systems using neural networks-based integrated intelligent computing. Neural Comput Appl 31(3):793–812